ELSEVIER

Earth and Planetary Science Letters 202 (2002) 201–216

EPSL

www.elsevier.com/locate/epsl

Analyses of nitrogen and argon in single lunar grains: towards a quantification of the asteroidal contribution to planetary surfaces

Ko Hashizume [a,b,*], Bernard Marty [b,c], Rainer Wieler [d]

[a] *Department of Earth and Space Sciences, Osaka University, Toyonaka, Osaka 560-0043, Japan*
[b] *CRPG-CNRS, P.O. Box 20, 54501 Vandoeuvre-lès-Nancy Cedex, France*
[c] *Ecole Nationale Supérieure de Géologie, 54501 Vandoeuvre-lès-Nancy Cedex, France*
[d] *Institute for Isotope Geology and Mineral Resources, ETH Zurich, NO C61, CH-8092 Zurich, Switzerland*

Received 16 April 2002; received in revised form 13 June 2002; accepted 19 June 2002

Abstract

We performed nitrogen and argon isotopic analyses in single 200-μm-sized ilmenite grains of lunar regolith samples 71501, 79035 and 79135. Cosmogenic and trapped components were discriminated using stepwise heating with a power-controlled CO_2 laser. Cosmogenic ^{15}N and ^{38}Ar correlate among different ilmenite grains, yielding a mean $^{15}N_c/^{38}Ar_c$ production ratio of 14.4 ± 1.0 atoms/atom. This yields a ^{15}N production rate in bulk lunar samples of 3.8–5.6 pg (g rock)$^{-1}$ Ma^{-1}, which agrees well with previous estimates. The trapped $\delta^{15}N$ values show large variations (up to 300‰) among different grains of a given soil, reflecting complex histories of mixing between different end-members. The $^{36}Ar/^{14}N$ ratio, which is expected to increase with increasing contribution of solar ions, varies from 0.007 to 0.44 times the solar abundance ratio. The trapped $\delta^{15}N$ values correlate roughly with the $^{36}Ar/^{14}N$ ratios from a non-solar end-member characterized by a $^{36}Ar/^{14}N$ ratio close to 0 and variable but generally positive $\delta^{15}N$ values, to lower $\delta^{15}N$ values accompanied by increasing $^{36}Ar/^{14}N$ ratios, supporting the claim of Hashizume et al. (2000) that solar nitrogen is largely depleted in ^{15}N relative to meteoritic or terrestrial nitrogen. Nevertheless, the $^{36}Ar/^{14}N$ ratio of the ^{15}N-depleted (solar) end-member is lower than the solar abundance ratio by a factor of 2.5–5. We explain this by a reprocessing of implanted solar wind atoms, during which part of the chemically inert rare gases were lost. We estimate that the flux of non-solar N necessary to account for the observed $\delta^{15}N$ values is comparable to the flux of micrometeorites and interplanetary dust particles estimated for the Earth. Hence we propose that the variations in $\delta^{15}N$ values observed in lunar regolith can be simply explained by mixing between solar wind contributions and micrometeoritic ones infalling on the Moon. Temporal variations of $\delta^{15}N$ values among samples of different antiquities could be due to changes in the micrometeoritic flux through time, in which case such flux has increased by up to an order of magnitude during the last 0.5 Ga.

Keywords: solar wind; N-15/N-14; Moon; regolith; micrometeorites

* Corresponding author. Tel.: +81-6-6850-5497; Fax: +81-6-6850-5541.
E-mail address: kohash@ess.sci.osaka-u.ac.jp (K. Hashizume).

0012-821X/02/$ – see front matter
PII: S0012-821X(02)00781-1

1. Introduction

The surface of the Moon has been exposed over billions of years to irradiation by solar ions, as evidenced by implanted solar rare gases in the lunar regolith, and to contributions of various extraterrestrial sources, as shown by the occurrence of 1–2% chondrite-like material in the lunar regolith [1]. Potential contributors include interplanetary dust particles (IDPs) and micrometeorites which dominate the present-day mass flux of meteoritic matter to the Earth's surface [2,3], meteorites and comets. In contrast to the Earth's surface, the lack of igneous activity since 3 Ga and of weathering on the Moon's surface together with the depletion of volatile elements in the Moon has allowed the preservation of the record of such contributions for highly volatile elements such as H, C, N and rare gases. Therefore, lunar regolith samples provide a unique opportunity to investigate the sources of impactors in the terrestrial region as well as possible secular variations of the respective fluxes.

As stated above, rare gases in the lunar regolith are dominated by the contribution from the Sun. The situation is potentially different for H, C and N which, scaled to rare gases, are enriched by several orders of magnitude in planetary materials relative to the Sun. Consequently, these elements are particularly suitable to investigate the nature of past fluxes of such materials. The abundance of nitrogen correlates fairly well with that of rare gases among different regolith samples (e.g., [4]), suggesting that this element has been implanted at the surface of regolith grains similar to solar wind (SW) rare gases. However, the isotopic composition of nitrogen ($^{15}N/^{14}N$) in lunar dust samples varies by up to 30% on a Ga time scale (e.g., [4–9]), despite the near-constancy of rare gas isotopic ratios [10–12]. This observation has been attributed to a secular variation in the N isotope composition of the solar corpuscular irradiation (e.g., [4–6] and references therein). This possibility was discarded by Geiss and Bochsler [13] on the ground that no known spallation or thermonuclear reaction could produce enough ^{15}N, and these authors concluded that the N isotope ratio at the solar surface has been constant during the last four billion years. They instead proposed that variations of the $^{15}N/^{14}N$ ratio are due to mixing between a ^{15}N-rich solar component and a very light planetary N component admixed in various amounts to the lunar regolith. The opposite mixing relationship, i.e., a mixture between a ^{15}N-poor solar component and a ^{15}N-rich heavy planetary N component, the case we propose in this paper with quantitative evidences, has been evaluated previously but was discarded (e.g., [6]) due to lack of supporting evidence.

The analysis of the N abundance together with that of Ar isotopes in single lunar regolith grains by laser extraction-static mass spectrometry developed in Nancy showed that the lunar regolith contains two or more nitrogen components [14]. To investigate the complex lunar nitrogen archive, we have performed a series of microscopic N isotopic analyses at CRPG, Nancy, aiming to characterize the possible N end-members [15]. Using a newly developed ion probe rastering method, we identified several N components at different depths in individual regolith grains. For Apollo 17 regolith breccia 79035, a light N component ($\delta^{15}N$ as low as $-240‰$ [15], where $\delta^{15}N \equiv \{[(^{15}N/^{14}N)_{sample}/(^{15}N/^{14}N)_{terrestrial\ air}]-1\}\cdot 1000$) was found within a depth range of 100 nm. This component is associated with D-free H, a strong indication of a solar origin. For another Apollo 17 regolith sample 71501, another N end-member was observed, characterized by enrichment in ^{15}N (up to $+70‰$ [8]) and associated with D-rich H [15]. This end-member was attributed to a nitrogen component derived from planetary bodies [15].

The relationship between planetary and solar components, however, is not straightforward. There does not exist a single elemental and isotopic mixing correlation for N and rare gases among different lunar regolith samples [4,8]. This requires either (i) contributions of different non-solar components having different isotopic compositions, (ii) fractionation of N relative to rare gases in the lunar regolith, (iii) variations in the contributing corpuscular fluxes over time, or (iv) a combination of these processes. The lunar regolith consists of a myriad of mineral grains and each of the grains may have a different pro-

cessing history. Instead of analyzing bulk samples as was mainly done in the past 30 yr, our approach has been to analyze N and Ar elemental compositions in single mineral grains from a few well-characterized regolith samples [14]. In this study, we expanded this approach to analyzing N and Ar isotopic compositions in single grains, combined with a stepwise heating technique to discriminate different isotopic components present in the grains. We have analyzed single ~200-μm-sized ilmenite grains from Apollo 17 samples 71501, 79035 and 79135. The $^{40}Ar/^{36}Ar$ ratios [16] as well as other maturity/antiquity indices suggest that 71501 has been exposed to the Moon's surface during the past 100 Ma, while the other two samples were presumably irradiated 1–2 Ga ago [17]. We will refer to these samples as 'recent' and 'old', respectively.

2. Experimental protocols and data analysis

At CRPG, Nancy, a mass spectrometry system has been developed capable of precisely determining the isotopic composition of N and Ar (^{38}Ar and ^{36}Ar) contained in a single ~200-μm-sized lunar grain in up to four temperature steps. Only the outline of the system is explained here, as the full details are published elsewhere [14,18,19].

The gas was extracted from single grains with a CO_2 laser (wavelength 10.6 μm) in continuous mode. The minimized area heated by the laser allowed us to obtain blank levels as low as 0.2 pmol N_2 (in vacuum pyrolysis mode) or 0.7 pmol N_2 (in combustion mode). The N blank level improved several-fold during this study [19]. Grains whose code starts with a letter (see **Background Data Set**[1] online tables), i.e., >80% of the ~200-μm-sized grains, were measured with the lowest blanks noted above. The ^{36}Ar blanks were typically in the range of 0.05–0.1 fmol. Stepwise analyses were performed by controlling the power of the laser. Although the temperature control is not accurate (presumably around 100°C), we could identify different gas components at different temperatures, as shown in Section 3. Samples were heated either in an oxygen atmosphere (P_{O_2} ~0.1 torr) or in vacuum, but both extraction modes yielded very similar gas release profiles. Extracted gases split into N_2 and Ar fractions were introduced into the mass spectrometer after impurities had been removed by standard protocols described in [14,18,19].

The isotopic compositions of N_2 and Ar were measured by a gas mass spectrometer (VG5400, Micromass©). When 0.4 pmol of N_2 was introduced into the mass spectrometer, the isotopic ratio ($^{15}N^{14}N/^{14}N^{14}N$) was determined with a precision typical of ±4‰ (1σ), which corresponds to the limit imposed by counting statistics [19]. Overall, our nitrogen isotopic analyses yielded a precision of about ±10‰ for typical N_2 amounts of ~1 pmol. The $^{38}Ar/^{36}Ar$ and $N_2/^{36}Ar$ ratios for the standard gas were reproduced within a precision of ~1% and 5–10%, respectively, for ~1 fmol of ^{36}Ar or ~1 pmol of N_2.

2.1. Component deconvolution

From the observed isotopic compositions of N and Ar, the amounts of cosmogenic and trapped components, respectively, were calculated assuming a binary mixing. The concentration of cosmogenic ^{38}Ar was calculated assuming that the $^{38}Ar/^{36}Ar$ ratio of the cosmogenic component is 1.59, and that of the trapped component is intermediate between the SW isotopic ratio (0.182 ± 0.002 and 0.185 ± 0.002 estimated for samples 71501 and 79035, respectively [11]) and the solar energetic particle (SEP) isotopic ratio (0.205 ± 0.002 and 0.196–0.206 for samples 71501 and 79035, respectively [11]). The final 2σ uncertainties of the concentrations of cosmogenic and trapped components take into account the range of possible values for the trapped component.

The cosmogenic ^{15}N concentration was calculated assuming that the trapped $\delta^{15}N$ values are −20‰ and −175‰ for samples 71501 and 79035/79135, respectively. These are the values assumed by [9] as the spallation-free N isotopic compositions of the trapped components released at relatively high temperatures. As in the case of

[1] http://www.elsevier.com/locate.epsl

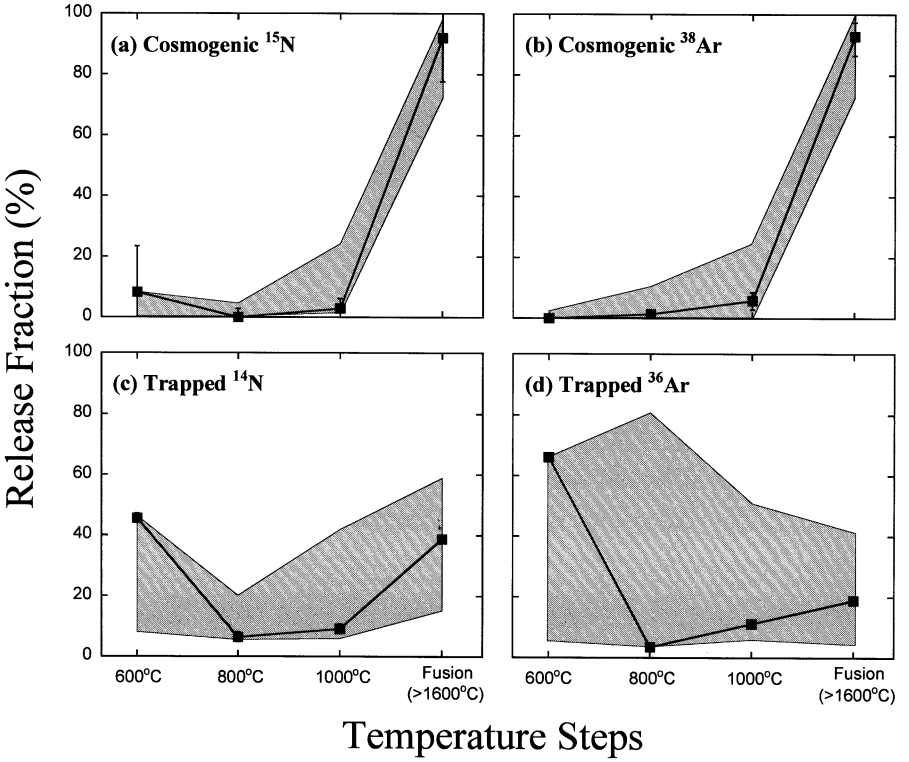

Fig. 1. Release of cosmogenic and trapped N and Ar components plotted against the heating temperature. Nine grains heated in four temperature steps are shown, whereas the rest of the grains were heated in two or three temperature steps. A typical case (71501 grain '3F') is plotted in solid squares. For the rest of the grains, the ranges of fractions released at the respective temperatures are shown in shaded areas.

Ar, we adopt a large error bar (± 150‰, 2σ) for the assumed trapped values, roughly covering the entire range of δ^{15}N values observed at non-fusion temperature steps (where the trapped N is released) by the stepwise heating experiment [8,9].

3. Results

Nitrogen and argon isotopic compositions of 44 ilmenite grains (32, 7 and 5 grains of samples 71501, 79035 and 79135, respectively) were measured, including the ones shown in [20]. About 80% of the grains were in the size range of 175–250 μm and had masses of approximately 0.04 mg, although some grains were considerably larger (up to 1 mg). The numeric data are given in **Background Data Set**[1], Tables 1–3. Table 1 (**Background Data Set**[1]) contains the full data of the stepwise analyses (N and ^{36}Ar abundances, δ^{15}N values and ^{38}Ar/^{36}Ar ratios), whereas Tables 2 and 3 (**Background Data Set**[1]) show the selected data used to draw the figures.

Gases were extracted in two to four temperature steps. Fig. 1 shows N and Ar release profiles of the trapped and cosmogenic components for grains analyzed in four steps. The figure demonstrates that trapped and cosmogenic nitrogen are fairly well discriminated. The former is mainly (40–95%) released below 1000°C and the latter mostly (70–100%) in the final fusion step (>1600°C). In the discussion hereafter, we use data for fractions which show δ^{15}N values higher than +100‰ (that is, the fusion steps for 27 grains and the 1000°C step for four grains) to study the cosmogenic component (**Background**

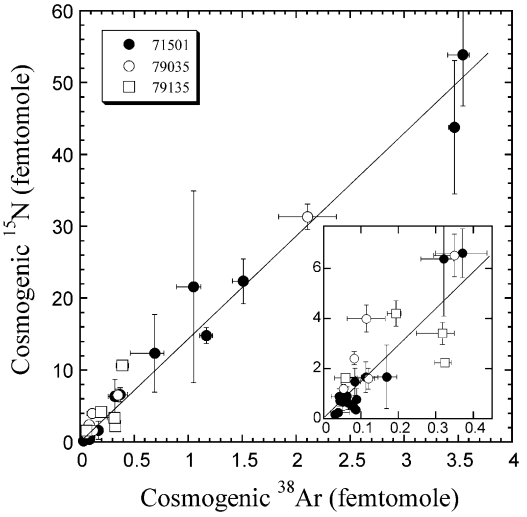

Fig. 2. Correlation between amounts of cosmogenic ^{15}N and co-released cosmogenic ^{38}Ar in Apollo 17 ilmenite grains. An enlarged diagram around the origin is shown in the inset. All fractions that show δ^{15}N values higher than +100‰ are selected for this plot. Most data points represent the fusion step, but four points are for the 1000°C step. There is no systematic difference in the proportion of the two cosmogenic nuclides between the fusion and 1000°C step data. Error bars represent 1σ errors. Uncertainties assumed for the isotopic ratios of the trapped components are included in the error bars. A mean production rate ratio (P_{15}/P_{38}) of 14.4 ± 1.0 atoms/atom is derived from the best-fit line. The correlation factor is 0.97.

Data Set[1], Table 2), and the low temperature (≤ 1000°C) step data to study the trapped component after corrections for minor cosmogenic contributions at these steps (**Background Data Set**[1], Table 3).

The mean values of the trapped component obtained here agree well with literature values. The abundance-weighed mean N/^{36}Ar ratios and δ^{15}N values of the ~200-μm-sized 71501 grains (22 grains) are 243 ± 5 and +1 ± 5‰, respectively, whereas the corresponding values obtained by a stepwise heating experiment of ~30 mg of fine ilmenite grains [8] are 294 and +14‰, respectively. (The literature values are the averages of the respective 400–1100°C steps.) This agreement suggests that contribution of contamination N that was anticipated to some degree seems to be not fatal. The ~200-μm-sized grains of sample 79035 also show good agreement with literature values, considering that only six grains were analyzed here. Our N/^{36}Ar ratios and the δ^{15}N values are 402 ± 18 and −96 ± 11‰, respectively, whereas [9] reports corresponding values of 699 and −78‰, the averages taken from their 400°C (pyrolysis) to 1100°C step data.

The basic characteristics observed by [14] regarding elemental abundances of N and ^{36}Ar in single lunar ilmenite grains were well reproduced in this study. The ^{36}Ar/N ratios were variable among grains and systematically lower than the solar abundance ratio (^{36}Ar/N = 0.0272 [21]). In our study the ^{36}Ar/N ratios ranged from 0.007 to 0.44 times the solar ratio (**Background Data Set**[1], Table 3), whereas [14] reported a range between 0.002 and 1. A general trend of ^{36}Ar/N being higher (closer to solar) with increasing ^{36}Ar abundance was seen both in this study and in [14].

4. Discussion

4.1. Cosmogenic nitrogen

In this study, the δ^{15}N values varied in a range of −200‰ to +2700‰. The highest values are observed mostly in fusion steps, and are due to cosmogenic nitrogen (^{15}N/^{14}N ~ 1). A good linear correlation between the amounts of cosmogenic ^{15}N and ^{38}Ar was obtained (Fig. 2) from which we are able to calculate the production rate ratio of these two nuclides. The best-fit line in Fig. 2 suggests a mean production rate ratio $^{15}N_c/^{38}Ar_c$ = 14.4 ± 1.0 atoms/atom for our lunar ilmenite grains. The average $^{15}N_c/^{38}Ar_c$ ratio for the four 1000°C step data is 13.1 ± 1.8 atoms/atom, whereas the corresponding value for the fusion (> 1600°C) step is 16.0 ± 7.4, suggesting that there is no significant difference between these temperature steps. We assume that the mean $^{15}N_c/^{38}Ar_c$ ratio is constant among all temperature steps and samples, and use the value of 14.4 atoms/atom to correct for the contribution of ^{15}N from the amount of $^{38}Ar_c$ estimated for each temperature step. We assign a rather conservative error of 33% (1σ) error on the adopted P_{15}/P_{38} ratio (to correct the low-temperature data dis-

cussed in Section 4.2), instead of the error for the best estimate value, reflecting the scatter among individual grains.

We can derive the $^{15}N_c$ production rate (P_{15}) if we have an estimate for the $^{38}Ar_c$ production rate ($P_{38,ilmenite}$) in our ilmenites. There are two approaches to do so: from nuclear physical models (e.g., [22,23]), or from direct measurements of ilmenite concentrates from lunar rocks (e.g., [24]). (i) Cosmogenic ^{38}Ar production by galactic cosmic rays (GCR) from parent nuclides Fe and Ti [22], $P_{38,ilmenite}$ is estimated to be rather constant at $\sim$20 fmol g^{-1} Ma^{-1} between the topmost surface and a depth of 40 g cm^{-2}. (We will not discuss the contribution of solar cosmic rays (SCR), because SCR-produced rare gases in a well-mixed regolith amount at best to a few percent of the GCR fraction [22], and we expect that this is not very different for nitrogen.) At greater depths, $P_{38,ilmenite}$ decreases roughly at a rate of 7×10^{-3} cm^2 g^{-1}. A recent estimate by [23] gives $\geq$50% higher rates for the ^{38}Ar production rate from Fe, but we cannot estimate the $P_{38,ilmenite}$ from their data because the ^{38}Ar production rate from Ti is not given. (ii) From a $^{38}Ar_c$ concentration of 28.5×10^{-8} cm^3 STP g^{-1} and a ^{81}Kr–Kr age of 350 Ma in an ilmenite concentrate (>95% ilmenite) of lunar rock 10071 [24], a ^{38}Ar production rate of 36 fmol g^{-1} Ma^{-1} can be computed. K-bearing minerals might have slightly contaminated the ilmenite concentrate ([K]$\sim$1400 ppm), as inferred from the high concentration of radiogenic ^{40}Ar. Since $^{38}Ar_c$ is produced 5–30 times more efficiently from K than from Ti [22], 2–11% of the $^{38}Ar_c$ in the ilmenite fraction might have derived from the K-bearing minerals. Taking into account such a contribution (and possibly also one from Ca present in impurities as well), the $P_{38,ilmenite}$ from the data of [24] might be quite similar to the modeled value of [22]. Therefore, we adopt the estimate of [22] as the absolute $P_{38,ilmenite}$ value used in this study. Within the typical range of the average shielding depth estimated for the lunar regolith samples, i.e., at 0–80 g cm^{-2}, $P_{38,ilmenite}$ is calculated to be between 14–20 fmol g^{-1} Ma^{-1}.

Consequently, the average production rate of cosmogenic ^{15}N for the Apollo 17 ilmenite grains studied here is calculated to be 200–290 fmol g^{-1} Ma^{-1}, from the possible range of $P_{38,ilmenite}$ at 0–80 g cm^{-2} and the average $^{15}N_c/^{38}Ar_c$ ratio obtained here. However, the production rates of cosmogenic ^{38}Ar and ^{15}N may depend differently on the burial depth. The model of [23], comparing the depth profile of the production rates of ^{14}C from O and ^{36}Cl from Ti or Fe, allows us to expect that $^{15}N_c$ is relatively more efficiently produced at larger shielding than $^{38}Ar_c$. If this is taken into account, the above-mentioned range of $P_{15,ilmenite}$ might be narrower. The concentration of O, the dominant target element for $^{15}N_c$ production, in ilmenite with stoichiometric elemental composition is 31.6 wt%, whereas the O concentration of lunar rocks is around 40 wt%. Therefore, the absolute cosmogenic ^{15}N production rate in bulk lunar rocks is estimated to be 250–370 fmol g^{-1} Ma^{-1}, or 3.8–5.6 pg ^{15}N g^{-1} Ma^{-1}. This estimate is comparable to the previous estimates of 5.8 ± 0.6 pg g^{-1} Ma^{-1} [25], of 4.1 pg g^{-1} Ma^{-1} (1.7–4.4 pg g^{-1} Ma^{-1} among different rocks) [26] and of 3.6 ± 0.8 pg g^{-1} Ma^{-1} [7].

4.2. Trapped nitrogen

In the 600–1000°C steps, large amounts of solar ^{36}Ar and ^{38}Ar were released (Fig. 1), together with nitrogen with variable $\delta^{15}N$ values. These steps represent, after corrections for cosmogenic contributions, the database for investigating the nature of the trapped components. The amounts of cosmogenic ^{15}N released at the non-fusion steps of individual grains are estimated from the amounts of co-released cosmogenic ^{38}Ar using the production rate ratio P_{15}/P_{38} obtained in this study.

In many cases the measured $\delta^{15}N$ values needed to be corrected by only a few ‰, although in a few cases the correction amounts to >100‰. This correction is not a real problem, as even the largest uncertainties are much less than the overall spread. The $\delta^{15}N$ values for the trapped components range between <-300‰ to +30‰, which roughly covers the whole range seen by stepwise analyses of the 71501 and 79035 samples reported by [8] and [9]. The wide spread in the

trapped $\delta^{15}N$ values and $^{36}Ar/N$ ratios among grains suggests that each grain has sampled multiple N and Ar components of different origins in various proportions.

First, we briefly characterize the possible end-member nitrogen components trapped in the lunar regolith. (i) Hashizume et al. [15] concluded that the $\delta^{15}N$ value for the trapped SW component is lower than $-240‰$ from ion probe depth profiling analysis. This result is compatible with recent reports on the nitrogen isotopic composition of the Jovian atmosphere, another source of information for the solar composition. Owen et al. [27] recently reported a $\delta^{15}N$ value of $-370 \pm 80‰$ measured by the Galileo probe mass spectrometer, in agreement with the measurement by the ISO probe ($-480^{+240}_{-280}‰$) [28]. Note that Kallenbach et al. [29] reported a $\delta^{15}N$ value of $+360^{+520}_{-290}‰$ for SW N measured by the SOHO probe. This latter value largely disagrees with the other three determinations. Here we therefore assume that the true solar value is within the range of -240 to $-450‰$. (ii) Planetary-type components should generally be depleted in ^{36}Ar relative to N (e.g., $(^{36}Ar/N)_{chondrite} < 10^{-5} \cdot (^{36}Ar/N)_{solar}$ [30]) and the corresponding $\delta^{15}N$ values should be higher than solar (e.g., $-100 < \delta^{15}N_{chondrite} < +1000‰$; references in [15]). (iii) The HCN of the comet Hale–Bopp seems to possess an intermediate $\delta^{15}N$ value of $-160 \pm 170‰$ [31] between the chondritic range and the solar value. The ^{15}N-depleted solar N proposed here is also consistent with this cometary value, since protosolar N is expected to be lighter than interstellar HCN produced by ion-molecule exchange reactions [32].

In Fig. 3, the $\delta^{15}N$ values of single grains are plotted against the $^{36}Ar/N$ ratios normalized by the solar abundance ratio. For a binary mixture of N and Ar components with constant $\delta^{15}N$ values and $^{36}Ar/N$ ratios, the mixing trend should be a single line in this diagram. If several non-solar end-members exist, no single correlation should be observed, but taking into account that the planetary $\delta^{15}N$ values are systematically higher than the solar value, a broadly negative correlation between $\delta^{15}N$ values and $^{36}Ar/N$ ratios would nevertheless be expected. (Though there exists a model that proposes terrestrial derivation of the light lunar N [33], we consider this to be unlikely, because any correlation with the solar H, like that observed in [15], should not be expected.) In general, data in Fig. 3 indeed exhibit such a mixing trend. Among the three samples, the 79035 ilmenite grains show the simplest and clearest trend. A negative correlation (correlation coefficient: 0.93) between the $\delta^{15}N$ values and the $^{36}Ar/N$ ratio can be explained by a binary mixing of two end-members, a ^{36}Ar-rich one with a $\delta^{15}N$ value lower than about $-240‰$ and a ^{36}Ar-poor one with a $\delta^{15}N$ value as high as $-70‰$. It is important to note that the $^{36}Ar/N$ ratio of the ^{36}Ar-rich end-member, which should be closely related to the solar component, seems to be significantly lower than the solar abundance ratio. The respective $^{36}Ar/N$ ratio deduced from the 79035 data array is estimated to be 0.2–0.4 times the solar abundance ratio, assuming that the $\delta^{15}N$ value of the ^{36}Ar-rich end-member is within the possible solar range of -240 to $-450‰$. Also, for sample 71501 the best-fit line has a negative slope, suggesting that

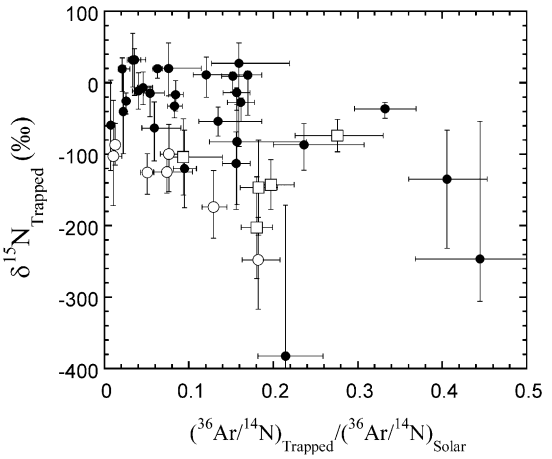

Fig. 3. The trapped $\delta^{15}N$ values for Apollo 17 single ilmenite grains plotted against the $^{36}Ar/N$ ratio normalized by the solar abundance ratio (0.0272 [21]). Data are taken from the non-fusion ($\leq 1000°C$) steps, where contributions of cosmogenic N are relatively small. Average values of the non-fusion step data are plotted. The trapped $\delta^{15}N$ values are obtained by subtracting cosmogenic ^{15}N from the measured $\delta^{15}N$ values using the estimated abundances of cosmogenic ^{38}Ar and the production rate ratio (P_{15}/P_{38}) obtained in this study.

the solar component trapped by this sample is depleted in ^{15}N, although a large scatter of the respective data (correlation coefficient: 0.55) makes it difficult to precisely specify the end-members. The data for 71501 grains, which generally plot in Fig. 3 at higher $^{36}Ar/N$ than the trend line for 79035 grains, suggest that the $^{36}Ar/N$ ratio of the solar component in 71501 might be closer to the true SW abundance ratio. We expect that such a difference in the solar $^{36}Ar/N$ ratio is likely to occur between immature samples like 71501 and mature samples like 79035. (See Section 4.3 for details.)

Lunar regolith samples show systematically lower $^{36}Ar/N$ ratios than the solar value (e.g., [4]), an observation taken by [14] to be due to addition of non-solar N. In this study, we confirm this argument based on the general picture displayed by our single grain data (Fig. 3). A large fraction of grains show $\delta^{15}N$ values higher than the solar value and $^{36}Ar/N$ ratios an order of magnitude lower than the solar abundance ratio. However, the present data suggest that the N enrichment is caused not only by non-solar components, but also because the $^{36}Ar/N$ ratio of the trapped solar component is significantly lower than the solar abundance ratio, at least in sample 79035. Due to the similarity in the first ionization potential between N and Ar, these two elements should not fractionate drastically in the solar corpuscular emissions relative to the solar abundance (i.e., $(^{36}Ar/N)_{SW} \sim (0.7–0.8)\cdot(^{36}Ar/N)_{Solar}$) [34]. Therefore, the only possible explanation for the N enrichment of the trapped SW component is the preferential loss of solar Ar from lunar samples. However, [17] concluded that such loss is unlikely to have taken place by diffusion-like processes, by which a mass-dependent fractionation is expected to occur because single lunar grains from the same regolith sample show constant relative abundances of Ar, Kr and Xe, irrespective of the absolute concentrations.

4.3. *A working hypothesis on the implantation mechanism of solar gases to the lunar mineral grains*

To explain a preferential loss of solar ^{36}Ar relative to N of a factor of 2.5–5 without fractionating the abundance ratios among Ar, Kr and Xe, we propose the following three-stage SW recycling mechanism. We attribute the fractionation between N and heavy rare gases to differences in their chemistry, which will play an important role in stage III.

I. The SW with energies around 1 keV/nucleon is implanted onto grain surfaces. The trapping probability of ions with an energy of several keV or higher is considered to be unity [35]. Therefore, no fractionation of solar rare gases relative to nitrogen will occur at this stage.

II. As the surface of the mineral becomes saturated with SW, part of the implanted solar gases will be released by ion sputtering, a process probably also explaining the Na in the lunar atmosphere [36]. This 'saturation' effect was experimentally reproduced by implanting α-particles with a SW energy into rock-forming minerals such as ilmenite or olivine [37]. The amount of trapped ^4He reached saturation when the dose of α-particles exceeded 10^{16} ions cm^{-2}. This corresponds to a ^4He concentration of $\sim 10^{-1}$ cm^3 STP g^{-1} in 100-μm-sized grains and is strikingly similar to the observed ^4He concentrations in lunar samples (e.g., 1.5×10^{-1} cm^3 STP g^{-1} in 100–150-μm-sized ilmenite grains of sample 71501 [8]). Therefore, the experiment of [37] suggests that at least the major gaseous elements might have become saturated at the lunar surface. The concentration of heavy rare gases trapped in size-sorted grains of mature lunar samples (e.g., ilmenite fraction of sample 79035 [9]) can be explained by a saturation model assuming a balance between acquisition and loss of gases at the mineral's implantation layer. Loss and gain are proportional to the concentration of the gas in the layer and the elements' abundance in the SW, respectively. We modelled that the mineral surface is sputtered off by a constant rate. Thereby, trapped gases are released, whereas the condensable elements will be redeposited at the grain surface.

III. The solar gases lost by sputtering form a dilute and transient atmosphere. The life time

of atmospheric Ar, for example, is estimated to be 80–100 days, whereas H and He which are not gravitationally bound to the Moon are lost within ~2 days [38]. The atmospheric species are ionized and re-implanted into the grains by the so-called Manka–Michel process [39]. The energy of the re-implanted ions is expected to be substantially low (0.1–1 keV per ion [39]) compared to the original SW, and their implantation probability must be lower than unity [40]. At such a low energy range, the implantation probability may be expected to depend on the chemical nature of the elements to be implanted. Nitrogen is likely to be chemically bound to silicates at very reducing conditions like those prevailing on the Moon's surface [41], and could therefore be trapped more efficiently than the chemically inert rare gases. Chemisorption of atmospheric species at mineral surfaces that are activated by implantation of high energy ions possibly plays a similar role here. Atmospheric nitrogen may react with cations such as silicon or titanium which have free radicals, while rare gases may remain in the atmosphere to be finally lost in space. We consider that any process whose kinetic energy delivered to the mineral surface does not dramatically exceed the binding energy of the (N-bearing) chemical compounds (<10 eV, inferred from the free energy of formation of TiN or Si_3N_4) is viable.

If part of the solar gases trapped in the regolith are recycled, one might expect a multi-modal distribution of the solar gases at variable depths in a grain. The re-implanted components with an energy of $\ll 1$ keV should be preferentially implanted at depths of <5 nm [35], the directly implanted SW with an energy of 1 keV/nucleon should reside at 30–100 nm [15,35], and SEP components should be at several hundred nm. However, such a distinct depth distribution could be perturbed by recoil effects of freshly implanted ions [35], which will displace already present ions to deeper locations. The deeper-than-expected distribution of the parentless ^{40}Ar observed among lunar samples supports such a remobilization. In stepwise pyrolysis or stepwise etching experiments, parentless ^{40}Ar is released at temperatures similar to solar ^{36}Ar (e.g., [11,42]).

As pointed out by [14], elemental fractionation among Ar, Kr and Xe is anticipated to occur in the lunar atmosphere due to the differences in their scale heights and other parameters [39]. Although this appears to be incompatible with the observed constant and close-to-solar Ar/Kr and Kr/Xe ratios among single lunar grains [17,43], this problem is safely bypassed by our model, because we consider that the re-trapping efficiency of fractionated solar rare gases is low (though not perfectly zero, as attested from the existence of parentless ^{40}Ar). Therefore, the rare gases trapped in the lunar regolith consist primarily of the originally implanted SW, i.e., the fraction which was not sputtered off at stage II.

It is interesting to note that [44] postulate, like us, that nitrogen and possibly carbon in lunar regolith have been recycled. The systematically lower C/N ratio of the lunar regolith (~1.5; [5]), compared to the typical range for chondritic materials (of the order of 10, e.g., [30]) or the solar ratio (3.2; [21]), had been regarded as one the problems in determining the origin of lunar C and N. They argue that the C/N ratio in the lunar regolith does not necessarily correspond to the original composition of the source material, but instead has been significantly modified by preferential loss of methane (a molecule lighter than N_2) from the lunar atmosphere [44]. In such a case, the lunar $\delta^{13}C$ values (e.g., [45]) that are often observed to be significantly higher than those for bulk meteoritic carbon (e.g., [30]) might be an indication of isotopic fractionation that has taken place during such a process. (If so, we could speculate that the isotopic fractionation of N_2 by the same process would be much smaller than several tens per mil.)

4.4. *Association of solar and meteoritic N at the lunar surface*

An obvious candidate for the ^{15}N-enriched non-solar N component in the lunar regolith is meteoritic material falling onto the Moon. The contemporary flux of extraterrestrial material falling on Earth is dominated by cosmic dust whose

size distribution peaks at around 200 μm [2,3]. The $\delta^{15}N$ values of micrometeorites are positive (up to +200‰; [46]) and IDPs appear to contain N as abundantly as the most primitive carbonaceous chondrites (~1000 ppm) [47], and to be enriched in ^{15}N relative to the solar composition ($-90 < \delta^{15}N_{IDP} < +480$‰ [48]; +800‰ [49]). Therefore, cosmic dust grains fit our requirement as a possible source of the non-solar N trapped in the lunar regolith. (A quantitative justification for this hypothesis will be made in Section 4.5.) Here we study whether mixing of solar and meteoritic N and Ar can explain the observed trends between N/Ar and $\delta^{15}N$ values.

Microimpactors, falling to the lunar surface at at least the escape velocity of 2.4 km/s, will be melted or vaporized and their organic N will be destroyed and released to the lunar atmosphere. The meteoritic N may then be recycled/reimplanted as described above. The source and the trapping mechanism of the non-solar (micrometeoritic) N we propose here explains the general characteristics of the non-solar N trapped in the lunar regolith, summarized by [4,50]:

1. The non-solar (isotopically heavy) N is extracted at similar but slightly lower temperatures than the solar (isotopically light) N. This is expected if non-solar N resides at somewhat shallower depths in the grains due to its lower implantation energy. Such layered structure of N components with different $\delta^{15}N$ values was directly observed among 71501 grains by depth-profiling using SIMS [15].
2. Bulk N concentrations in regolith samples are roughly proportional to those of the heavy rare gases regardless of the N isotopic composition, although the N/rare gas abundance ratio is approximately 10 times higher than solar. This correlation was used by [4,50] as supporting evidence that the bulk of lunar N is of solar origin. This author also used this correlation to reject hypotheses involving large contributions of non-solar N, pointing out that SW irradiation and (sporadic) meteorite falls are independent events, and that therefore no correlation will be expected between the abundances of solar Ar and non-solar N. However, if we assume that the bulk of extraneous material is contributed by micrometeorites, this reservation does not hold [51]. We will now attempt to quantify the bulk $N/^{36}Ar$ ratio expected in our scenario.

We define the bulk $N/^{36}Ar$ ratio normalized to the solar abundance ratio as F. The bulk N consists of three components: directly implanted SW, recycled solar N and planetary (micrometeoritic) N, whereas for ^{36}Ar, the planetary component can be neglected. We define two parameters, one already discussed above. (a) The recycling fraction (f_R) is the fraction of the solar gas sputtered off at stage II. Therefore, the amount of directly implanted SW trapped in lunar dust is expressed as $(1-f_R)N_{SW}$, and that of recycled solar gas as $f_R N_{SW}$, where N_{SW} denotes the total amount of SW N contributed to the lunar regolith. (b) We argue that the re-trapping efficiency of recycled solar ^{36}Ar (ε) relative to N is much smaller than unity (i.e., $\varepsilon \ll 1$). The re-trapping efficiency of N could be somewhat smaller than unity, although it should not be negligibly small because, if so, non-solar N could not be trapped, leading to a uniform (solar) $\delta^{15}N$ value. For the sake of simplicity, the re-trapping efficiency of N is approximated to unity. We assume that the $^{36}Ar/N$ ratio of the SW, and for simplicity also that of the recycled solar gas, is the same as the solar abundance ratio. The amount of the directly implanted SW ^{36}Ar is therefore expressed as $(1-f_R)(^{36}Ar/N)_{Solar}N_{SW}$, and that of the recycled solar ^{36}Ar as $\varepsilon f_R(^{36}Ar/N)_{Solar}N_{SW}$. Consequently, the F value is expressed as follows:

$$F \equiv \frac{(N/^{36}Ar)_{Bulk}}{(N/^{36}Ar)_{Solar}} = \frac{N_{SW} + N_P}{(1-f_R)N_{SW} + \varepsilon f_R N_{SW}} \quad (1)$$

where N_P is the abundance of N supplied by micrometeorites. Here, we introduce a third parameter (f_P) which is defined as:

$$N_P = f_P N_{SW} \quad (2)$$

The parameter f_P essentially determines the bulk $\delta^{15}N$ value:

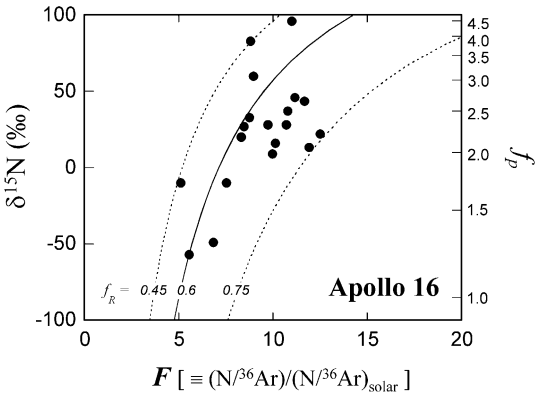

Fig. 4. Compilation of literature $\delta^{15}N$ and F values among bulk Apollo 16 regolith samples. (Data for mineral separates and size separates are excluded.) The f_P values, i.e., the mixing proportion of the two end-members, the solar and planetary components, are calculated by solving Eq. 3, assuming that their $\delta^{15}N$ values are −370‰ and +200‰, respectively. The three lines represent the theoretical curves given by Eq. 5 for the three cases of the recycling fraction (f_R) noted in the figure. The f_R values for the solid line are the same as the one we inferred in this study for sample 79035. The observed trend, i.e., the wide variation of the $\delta^{15}N$ values with fairly constant N/^{36}Ar ratios (differing only by a factor of 2.5 among different samples), can be easily explained by differences in the f_P values among samples, combined with a reasonably small fluctuation in the f_R values among them.

$$\delta^{15}N_{Bulk} = \frac{\delta^{15}N_{Solar} + f_P\delta^{15}N_P}{1+f_P} \quad (3)$$

where $\delta^{15}N$ values of the end-members (solar: $\delta^{15}N_{Solar}$, and planetary: $\delta^{15}N_P$) are discussed in Section 4.5. Using the parameter f_P, the F value is rewritten in simpler form as follows:

$$F = \frac{1+f_P}{1-f_R+\varepsilon f_R} \quad (4)$$

When the Ar re-trapping rate can be approximated to be zero, Eq. 4 becomes even simpler:

$$F = \frac{1+f_P}{1-f_R} \quad (5)$$

The observed correlation between bulk concentrations of N and ^{36}Ar (e.g., the case of Apollo 16 samples compiled in figure 1 of [4]) suggests that the F value is fairly constant regardless of the bulk $\delta^{15}N$ value. The literature F and $\delta^{15}N$ values for bulk Apollo 16 regolith samples are compiled in Fig. 4. Indeed, the F values show a narrow range within 5–13, while the bulk $\delta^{15}N$ values spreads between −60 to +100‰, with only a weak correlation between them. The three lines in the diagram represent our model (Eq. 5), assuming slightly different f_R values among them. Though [4,50] argues that one should expect a correlation between the F value and the $\delta^{15}N$ values if the $\delta^{15}N$ variation is due to different admixtures of non-solar N, it is not surprising that we do not observe such a correlation. This is because such a trend will easily be blurred due to small differences in the f_R value among the samples, which appear likely to occur, e.g., depending on the average maturity of the regolith around the sample location [51]. In Section 4.5, we propose that the f_P value had not been strictly constant over time, but showed a secular variation of at least one order of magnitude.

4.5. *Micrometeorite flux on the Moon and its secular variation*

In this study, we argue that two important sources supplied nitrogen to the lunar surface, micrometeorites and the SW, both possessing largely different isotopic compositions. With this hypothesis, the bulk $\delta^{15}N$ values for the trapped lunar N allow us to make a rough estimate of the f_P value defined above, i.e., the flux ratio of the solar and the micrometeoritic N.

The bulk $\delta^{15}N$ values of lunar regolith samples cover a wide range ($-170 < \delta^{15}N < +100$‰ [4]). This range is in between the possible solar range (−240 to −450‰) and the highest micrometeoritic values found in IDPs (+480 or +800‰; [48,49]). Although $\delta^{15}N$ values of individual IDPs and micrometeorites vary widely, an adequate $\delta^{15}N$ value to be assumed here as end-member of the planetary component should be, for example, the mean value of cluster IDPs of +140‰ [48] or the median value of numbers of

grains of +200‰ [48]. Partial resemblance of Antarctic micrometeorites to CM or CR chondrites, suggested from petrographic and geochemical studies [3,52], O isotope [53] and H isotope studies [54], also allows us to expect that micrometeorites are enriched in ^{15}N relative to the solar value because average $\delta^{15}N$ values of CM and CR chondrites are +40 and +200‰, respectively [30]. This range is indeed observed in Antarctic micrometeorites [46]. Assuming that the $\delta^{15}N$ values for the solar and micrometeorite end-members are −370‰ and +200‰, respectively, the bulk lunar $\delta^{15}N$ values suggest that 35–80% of the nitrogen originates from micrometeorites. Thus the supply rate of micrometeoritic N is 0.5–5 times that of the SW N.

The SW N flux supplied close to the sub-Earth point at the lunar surface (where the available documented lunar samples are from) is estimated to be $\sim 4\times10^3$ atoms cm^{-2} s^{-1}, from the SW proton flux of 2.8×10^8 atoms cm^{-2} s^{-1} [55], the solar abundance ratio ($N/H = 1.1\times10^{-4}$ [21]), and a shielding factor of 0.14 due to the rotation of the Moon and shielding by the terrestrial magnetosphere [56]. The supply rate of micrometeoritic N is therefore estimated to be $(0.2–2)\times10^4$ atoms cm^{-2} s^{-1}. If we assume that the N concentration of micrometeorites is the same as those of CM, CR chondrites and IDPs which contain ~1000 ppm of N [30,47], the accretion rate of micrometeorites on the Moon is estimated to be $(0.15–1.5)\times10^2$ g rock km^{-2} yr^{-1}. If the accretion rate on Earth is the same, this would correspond to $(0.75–7.5)\times10^4$ tons yr^{-1} of micrometeorites falling on Earth. Within this range, the upper limit corresponds to the estimate for recently exposed lunar regolith, such as sample 71501. This estimate is in striking agreement with the contemporary accretion rate of $40\,000\pm20\,000$ tons yr^{-1} estimated on direct measurements in near-Earth interplanetary space [2], although such a comparison neglects the different efficiencies of Earth and Moon to accrete interplanetary dust due to gravitational focusing. Gravitational focusing of IDPs may occur when the geocentric encounter velocity between particles and planets is smaller than the planet's escape velocity [57]. The flux of cometary dust that possesses high encounter velocity on Earth and the Moon should not differ, whereas the flux of asteroidal dust to Earth might be enhanced by a factor of 4–9 relative to that to the Moon. We roughly estimate that the total flux of IDPs to Earth might be higher than that to the Moon by a factor of ~3 (although it depends on the distribution of the encounter velocity among the particles). The upper limit of dust particle fluxes estimated for the Moon (this study) and for Earth [2], both corrected for the gravitational focusing effect, nevertheless show a remarkable agreement within a factor of 3–4.

A further argument for micrometeoritic contributions to the lunar surface comes from the amount of chondritic material present in lunar soils. If the micrometeorite accretion rate calculated above has been constant throughout the entire lunar history, the total amount of micrometeoritic material accumulated in the lunar regolith is 6–60 g rock cm^{-2}. Assuming that the average depth of the regolith is 10 meters, micrometeorites would contribute 0.4–4 wt%. This range agrees well with the estimate given by [1], of about 2 wt% of the regolith consisting of carbonaceous chondrite-type matter. Although contributions by large meteorites, especially during the heavy meteoritic bombardment period, have to be considered, this is independent evidence supporting our argument.

The inferred ~10-fold variation in the estimated flux of micrometeorites to the Moon is based on the variable $\delta^{15}N$ values in the lunar regolith. Although the estimated absolute accretion rates may be systematically biased due to the uncertainties of the above estimates, the deduced relative variations appear to be robust. We therefore propose that the observed trend between the trapped $\delta^{15}N$ values and the ^{38}Ar exposure age among single grains (Fig. 5) indicates a temporal variation of the micrometeorite accretion rate. Grains with a shorter cosmic-ray exposure age tend to show higher $\delta^{15}N$ values, whereas grains with a longer age show lower $\delta^{15}N$. This may be interpreted as a secular increase of the micrometeorite accretion rate during the last few hundreds of Ma. This view is in agreement with [58], who argue that the frequency of small impact events on the lunar surface increased by a factor

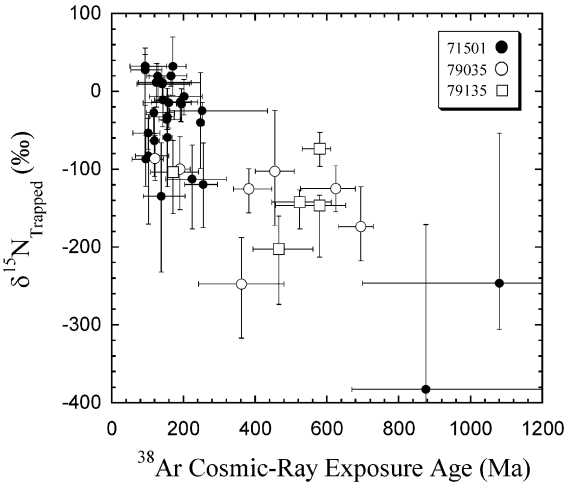

Fig. 5. The $\delta^{15}N$ values of trapped N plotted against the ^{38}Ar cosmic-ray exposure age for Apollo 17 single ilmenite grains. The trapped $\delta^{15}N$ values are the same as those plotted in Fig. 3. The ^{38}Ar cosmic-ray exposure age is calculated from the total concentration of cosmogenic ^{38}Ar in the respective grain. The absolute cosmogenic ^{38}Ar production rate of 19 fmol (g ilmenite)$^{-1}$ Ma^{-1} is uniformly applied to all grains. A similar trend between trapped $\delta^{15}N$ values and ^{21}Ne cosmic-ray exposure ages among bulk lunar samples was previously shown by [6], but was interpreted in a different way, as supporting evidence of the secular variation in the solar $\delta^{15}N$ value.

of 4 in the last 400 Ma, based on ^{40}Ar–^{39}Ar dating of individual lunar glass spherules, and with another study advocating an increase of the flux of extraterrestrial material on the Earth in the last few hundreds of Ma [59].

5. Summary and conclusions

The nitrogen isotopic composition in single 200-μm-sized lunar ilmenite grains from samples 71501, 79035 and 79135 has been analyzed along with the $^{38}Ar/^{36}Ar$ ratio using a high sensitivity gas mass spectrometer combined with a laser-assisted stepwise gas-extraction method. Cosmogenic and trapped components were extracted almost separately, allowing us to estimate the cosmogenic $^{15}N/^{38}Ar$ production ratio in lunar ilmenite grains from high-temperature gas fractions. This ratio – together with the measured $^{38}Ar/^{36}Ar$ ratio – was used to estimate the trapped $\delta^{15}N$ values in single grains by correcting the measured N composition in low-temperature steps for small amounts of cosmogenic ^{15}N.

1. Concentrations of the cosmogenic ^{15}N correlate well with those of the cosmogenic ^{38}Ar in all ilmenite grains. A production rate ratio of $^{15}N_c/^{38}Ar_c = 14.4 \pm 1.0$ atoms/atom was obtained. The cosmogenic ^{15}N production rate ratio in bulk lunar rocks shielded at a depth of 0–80 g cm^{-2} is calculated from the obtained production rate ratio to be 3.8–5.6 pg (g rock)$^{-1}$ Ma^{-1}, in good agreement with previous estimates.
2. A wide variation of the trapped $\delta^{15}N$ values of between 130‰ to >300‰ was observed among grains of the same regolith samples. The $^{36}Ar/^{14}N$ ratio was also observed to be variable and systematically lower than the solar abundance ratio, by 0.007–0.44 times, confirming the previous study by [14] and suggesting that non-solar (planetary-type) components contribute significantly to lunar nitrogen.
3. Grains with $^{36}Ar/^{14}N$ ratio closer to the solar abundance ratio tend to show lower trapped $\delta^{15}N$ values, supporting the argument by [15,27] that the solar nitrogen is largely depleted in ^{15}N relative to terrestrial or meteoritic nitrogen. Such a trend showed most clearly among the 79035 grains. The $^{36}Ar/^{14}N$ ratio of the ^{36}Ar-enriched end-member, presumably the solar component, is estimated to be 0.2–0.4 times the solar abundance ratio.
4. To explain the partial depletion of solar argon trapped in lunar regolith grains, we propose a reprocessing model of the solar gas implanted into the lunar regolith: solar ions once implanted into the lunar regolith are sputtered out by freshly implanted ions. These sputtered-off atoms form a dilute lunar atmosphere, from where they are re-implanted into the regolith with a lower energy than that of the SW. At this stage, nitrogen could be more efficiently trapped compared to less chemically active rare gases.
5. We argue here that the $\delta^{15}N$ variation observed among the lunar samples reflect mixing

in variable proportions of SW nitrogen and nitrogen derived from planetary materials, predominantly from micrometeorites. From the mixing ratio of the two nitrogen components, we estimate the flux of planetary material to the Moon to be within a range of (0.75–7.5)$\times 10^4$ tons yr^{-1}, depending on the exposure age of the regolith. The upper limit, derived from relatively recently exposed samples, is in good agreement with the directly measured contemporary micrometeoritic flux (40 000 ± 20 000 tons yr^{-1}) in near-Earth interplanetary space [2].

6. In our model, the secular $\delta^{15}N$ variations among individual regolith grains, or among different regolith samples, result from variations in the accretion rate of planetary material, a view consistent with independent arguments for an increase of the accretion rate of planetary material in the last ~0.5 Ga [58,59].

Acknowledgements

We are indebted to Laurent Zimmermann for his technical assistance. We thank Marc Chaussidon and Kurt Marti for stimulating discussions. We are grateful to R.H. Becker, S. Assonov and an anonymous reviewer for their constructive reviews. R.H. Becker is also acknowledged for providing us with his database of lunar nitrogen and argon data. K.H. thanks members of CRPG-CNRS for their hospitality during his stay. This study was supported by the Japanese Ministry of Education, Culture, Sports, Science and Technology, by CNRS for K.H. through a 'Poste Rouge' fellowship, by grants from INSU-PNP and from Région Lorraine, partly from the Mitsubishi Foundation, and from Grant-in-Aid for Encouragement of Young Scientists from JSPS (12740305). This work is CRPG-CNRS contribution 1594. *[RV]*

References

[1] J.W. Morgan, U. Krähenbühl, R. Ganapathy, E. Anders, Trace elements in Apollo 15 samples: implications for meteorite influx and volatile depletion on the Moon, Proc. Lunar Sci. Conf. 3rd, 1972, pp. 1361–1376.

[2] S.G. Love, D.E. Brownlee, A direct measurement of the terrestrial mass accretion rate of cosmic dust, Science 262 (1993) 550–553.

[3] C. Engrand, M. Maurette, Carbonaceous micrometeorites from Antarctica, Meteorit. Planet. Sci. 33 (1998) 565–580.

[4] J.F. Kerridge, Long-term compositional variation in solar corpuscular radiation: evidence from nitrogen isotopes in the lunar regolith, Rev. Geophys. 31 (1993) 423–437.

[5] J.F. Kerridge, Solar nitrogen: evidence for a secular increase in the ratio of nitrogen-15 to nitrogen-14, Science 188 (1975) 162–164.

[6] J.F. Kerridge, What has caused the secular increase in solar nitrogen-15?, Science 245 (1989) 480–486.

[7] R.H. Becker, R.N. Clayton, T.K. Mayeda, Characterisation of lunar nitrogen components, Proc. 7th Lunar Sci. Conf., 1976, pp. 441–458.

[8] U. Frick, R.H. Becker, R.O. Pepin, Solar wind record in the lunar regolith: nitrogen and noble gases, Proc. 18th Lunar Planet. Sci. Conf., 1988, pp. 87–120.

[9] R.H. Becker, R.O. Pepin, Long-term changes in solar wind elemental and isotopic ratios: a comparison of two lunar ilmenites with different antiquities, Geochim. Cosmochim. Acta 53 (1989) 1135–1146.

[10] R. Wieler, H. Baur, P. Signer, Noble gases from solar energetic particles revealed by closed system stepwise etching of lunar soil minerals, Geochim. Cosmochim. Acta 50 (1986) 1997–2017.

[11] J.-P. Benkert, H. Baur, P. Signer, R. Wieler, He, Ne, and Ar from the solar wind and solar energetic particles in lunar ilmenites and pyroxenes, J. Geophys. Res. 98 (1993) 13147–13162.

[12] R. Wieler, H. Baur, Krypton and xenon from the solar wind and solar energetic particles in two lunar ilmenites of different antiquity, Meteoritics 29 (1994) 570–580.

[13] J. Geiss, P. Bochsler, Nitrogen isotopes in the solar system, Geochim. Cosmochim. Acta 46 (1982) 529–548.

[14] R. Wieler, F. Humbert, B. Marty, Evidence for a predominantly non-solar origin of nitrogen in the regolith revealed by single grain analyses, Earth Planet. Sci. Lett. 167 (1999) 47–60.

[15] K. Hashizume, M. Chaussidon, B. Marty, F. Robert, Solar wind record on the Moon: deciphering presolar from planetary nitrogen, Science 290 (2000) 1142–1145.

[16] O. Eugster, D. Terribilini, E. Polnau, J. Kramers, The antiquity indicator $^{40}Ar/^{36}Ar$ for lunar surface samples calibrated by uranium-235-xenon-136 dating, Meteorit. Planet. Sci. 36 (2001) 1097–1115.

[17] R. Wieler, K. Kehm, A.P. Meshik, C.M. Hohenberg, Secular changes in the xenon and krypton abundances in the solar wind recorded in single lunar grains, Nature 384 (1996) 46–49.

[18] F. Humbert, G. Libourel, C. France-Lanord, L. Zimmermann, B. Marty, CO_2-laser extraction-static mass spectrometry analysis of ultra-low concentrations of nitrogen

in silicates, Geostand. Newsl.: J. Geostand. Geoanal. 24 (2001) 255–260.
[19] K. Hashizume, B. Marty, Nitrogen isotopic analyses at the sub-picomole level using an ultra-low blank laser extraction technique, in: P. de Groot (Ed.), Handbook of Stable Isotope Analytical Techniques, Elsevier Science, Amsterdam (2002), in press.
[20] K. Hashizume, B. Marty, R. Wieler, Single grain analyses of the nitrogen isotopic composition in the lunar regolith: in search of the solar wind component, Lunar Planet. Sci. Conf. XXX, 1999, Abstract #1567 (CD-ROM).
[21] E. Anders, N. Grevesse, Abundances of the elements: meteoritic and solar, Geochim. Cosmochim. Acta 53 (1989) 197–214.
[22] C.M. Hohenberg, K. Marti, F.A. Podosek, R.C. Reedy, J.R. Shirck, Comparisons between observed and predicted cosmogenic noble gases in lunar samples, Proc. Lunar Planet. Sci. Conf. 9th, 1978, pp. 2311–2344.
[23] I. Leya, S. Neumann, R. Wieler, R. Michel, The production of cosmogenic nuclides by GCR-particles for 2π exposure geometries, Meteorit. Planet. Sci. 36 (2001) 1547–1561.
[24] P. Eberhardt, J. Geiss, H. Graf, N. Grögler, U. Krähenbühl, H. Schwaller, A. Stettler, Noble gas investigations of lunar rocks 10017 and 10071, Geochim. Cosmochim. Acta 38 (1974) 97–120.
[25] K.J. Mathew, K. Marti, Lunar nitrogen: indigenous signature and cosmic-ray production rate, Earth Planet. Sci. Lett. 184 (2001) 659–669.
[26] D.J. DesMarais, Light element geochemistry and spallogenesis in lunar rocks, Geochim. Cosmochim. Acta 47 (1983) 1769–1781.
[27] T. Owen, P.R. Mahaffy, H.B. Niemann, S. Atreya, M. Wong, Protosolar nitrogen, Astrophys. J. 553 (2001) L77–L79.
[28] T. Fouchet, E. Lellouch, B. Bézard, T. Encrenaz, P. Drossart, H. Feuchtgrubert, T. de Graauw, ISO-SWS observations of Jupiter: measurement of the ammonia tropospheric profile and of the $^{15}N/^{14}N$ isotopic ratio, Icarus 143 (2000) 223–243.
[29] R. Kallenbach, J. Geiss, F.M. Ipavich, G. Gloeckler, P. Bochsler, F. Gleim, S. Hefti, M. Hilchenbach, D. Hovestadt, Isotopic composition of solar wind nitrogen: first *in situ* determination with the CELIAS/MTOF spectrometer on board SOHO, Astrophys. J. 507 (1998) L185–L188.
[30] J.F. Kerridge, Carbon, hydrogen and nitrogen in carbonaceous chondrites: abundances and isotopic compositions in bulk samples, Geochim. Cosmochim. Acta 49 (1985) 1707–1714.
[31] D.C. Jewitt, H.E. Matthews, T. Owen, R. Meier, Measurements of $^{12}C/^{13}C$, $^{14}N/^{15}N$, and $^{32}S/^{34}S$ ratios in comet Hale-Bopp (C/1995 O1), Science 278 (1997) 90–93.
[32] R. Terzieva, E. Herbst, The possibility of nitrogen isotopic fractionation in interstellar clouds, Mon. Not. R. Astron. Soc. 317 (2000) 563–568.
[33] J. Geiss, P. Bochsler, Long time variations in solar wind properties: possible causes versus observations, in: C.P. Sonett et al. (Eds.), The Sun in Time, Univ. Arizona, Tucson, AZ, 1991, pp. 98–117.
[34] J. Geiss, G. Gloeckler, R. vonSteiger, Solar and heliospheric processes from solar wind composition measurements, Philos. Trans. R. Soc. London Ser. A 349 (1994) 213–226.
[35] J.F. Ziegler, J.P. Biersack, U. Littmark, The Stopping and Range of Ions in Solids, vol. 1, Pergamon, New York, 1985.
[36] A.E. Potter, T.H. Morgan, Coronagraphic observation of the lunar sodium surface, J. Geophys. Res. 103 (1998) 8581–8586.
[37] T. Futagami, M. Ozima, Y. Nakamura, Helium ion implantation into minerals, Earth Planet. Sci. Lett. 101 (1990) 63–67.
[38] R.R. Hodges, Formation of the lunar atmosphere, Moon 14 (1975) 139–157.
[39] R.H. Manka, F.C. Michel, Lunar atmosphere as a source of lunar surface elements, Proc. 2nd Lunar Sci. Conf., 1971, pp. 1717–1728.
[40] F. Bühler, J. Geiss, J. Meister, P. Eberhardt, J.C. Hunecke, P. Signer, Trapping probability of the solar wind in solids. Part I. Trapping probability of low energy He, Ne, and Ar ions, Earth Planet. Sci. Lett. 1 (1966) 249–255.
[41] F. Humbert, Solubilité de l'azote dans les silicates liquides – Influence de la fugacité d'oxygène et de la composition, Thesis, Université Henri Poincaré, Nancy 1, France, 1998, 164 pp.
[42] R.O. Pepin, R.H. Becker, D.J. Schlutter, Irradiation records in regolith materials. I. Isotopic compositions of solar-wind neon and argon in single lunar mineral grains, Geochim. Cosmochim. Acta 63 (1999) 2145–2162.
[43] R. Wieler, H. Baur, Fractionation of Xe, Kr, and Ar in the solar corpuscular radiation deduced by closed system etching of lunar soils, Astrophys. J. 453 (1995) 987–997.
[44] S.S. Assonov, I.A. Franchi, C.T. Pillinger, A.S. Semenova, Yu.A. Shukolyukov, A.B. Verchovsky, A.N. Iassevitch, Nitrogen and argon release profiles in Luna-16 and Luna-24 regolith samples: the effects of regolith reworking, Meteorit. Planet. Sci. 37 (2002) 27–48.
[45] R.H. Becker, Evidence for a secular variation in the $^{13}C/^{12}C$ ratio of carbon implanted in lunar soils, Earth Planet. Sci. Lett. 50 (1980) 189–196.
[46] B. Marty, G. Matrajt, L. Zimmermann, C. Engrand, J. Duprat, Nitrogen and noble gas isotopes in Antarctic micrometeorites, Lunar Planet. Sci. Conf. XXXIII, 2002, Abstract #1578 (CD-ROM).
[47] L.P. Keller, K.L. Thomas, J.P. Bradley, D.S. McKay, Nitrogen in interplanetary dust particles, Meteorit. Planet. Sci. 30 (1996) 526–527 (Abstract).
[48] S. Messenger, Identification of molecular-cloud material in interplanetary dust particles, Nature 404 (2000) 968–971.
[49] F.J. Stadermann, Hydrogen, carbon and nitrogen isotopic imaging of sub-micron components from interstellar dust

particles, Lunar Planet. Sci. Conf. XXXII, 2001, Abstract #1792 (CD-ROM).
[50] J.F. Kerridge, Isotopic variability of nitrogen in lunar regolith – comment, Science 293 (2001) 1947a.
[51] K. Hashizume, M. Chaussidon, B. Marty, F. Robert, Isotopic variability of nitrogen in lunar regolith – response, Science 293 (2001) 1947a.
[52] G. Kurat, C. Koeberl, T. Presper, F. Brandstätter, M. Maurette, Petrology and geochemistry of Antarctic micrometeorites, Geochim. Cosmochim. Acta 58 (1994) 3879–3904.
[53] C. Engrand, K.D. McKeegan, L.A. Leshin, J.P. Bradley, D.E. Brownlee, Oxygen isotopic compositions of interplanetary dust particles: 16O-excess in a GEMS-rich IDP, Lunar Planet. Sci. Conf. XXX, 1999, Abstract #1690 (CD-ROM).
[54] C. Engrand, E. Deloule, F. Robert, M. Maurette, G. Kurat, Extraterrestrial water in micrometeorites and cosmic spherules from Antarctica: an ion microprobe study, Meteorit. Planet. Sci. 34 (1999) 773–786.
[55] A.J. Hundhausen, S.J. Bame, J.R. Ashbridge, S.J. Sydoriak, Solar wind proton properties: Vela 3 observations from July 1965 to June 1967, J. Geophys. Res. 75 (1970) 4643–4651.
[56] T.D. Swindle, M.K. Burkland, J.R. Johnson, S.M. Larson, R.V. Morris, B. Rizk, R.B. Singer, Systematic variations in solar wind fluence with lunar location: implications for abundances of solar-wind-implanted volatiles, Lunar Planet. Sci. Conf. XXIII, 1992, pp. 1395–1396 (Abstract).
[57] S.J. Kortenkamp, S.F. Dermott, D. Fogle, K. Grogan, Sources and orbital evolution of interplanetary dust accreted by Earth, in: B. Peuker-Ehrenbrink, B. Schmitz (Eds.), Accretion of Extraterrestrial Matter Throughout Earth's History, Kluwer Academic, Spuiboulevard, The Netherlands, 2001, pp. 13–30.
[58] T.S. Culler, T.A. Becker, R.A. Muller, P.R. Renne, Lunar impact history from $^{40}Ar/^{39}Ar$ dating of glass spherules, Science 287 (2000) 1785–1788.
[59] R.A.F. Grieve, E.M. Shoemaker, The record of past impacts on Earth, in: T. Gehrels (Ed.), Hazards Due to Comets and Asteroids, Univ. Arizona, Tucson, AZ, 1994, pp. 417–462.